A High-Resolution NMR Study of Long-Lived Water Molecules in Both Oxidation States of a Minimal Cytochrome *c*[†]

Ivano Bertini,*[,‡,§] Kaushik Ghosh,[‡] Antonio Rosato,[‡,§] and Paul R. Vasos[‡]

Magnetic Resonance Center (CERM), University of Florence, Via L. Sacconi 6, 50019 Sesto Fiorentino, Italy, and Department of Chemistry, University of Florence, Via della Lastruccia 3, 50019 Sesto Fiorentino, Italy

Received December 4, 2002; Revised Manuscript Received January 31, 2003

ABSTRACT: The interaction of water with oxidized and reduced cytochrome *c* from the Gram-positive bacterium *Bacillus pasteurii* (a 71-amino acid long monoheme cytochrome) is investigated through CLEANEX experiments and ^{15}N-edited ePHOGSY and Tr-ROESY experiments. It appears that a water molecule gives rise to dipolar cross-relaxation with the amide protons of Gly74 and Ile75, with a residence time longer than 0.4 ns, to account for a negative NOE. Such water molecule is present in both the oxidized and reduced species and in the X-ray structure. It appears to have a structural role. Other possible roles are discussed by comparison with the water molecules present in other *c*-type cytochromes. The amide proton of Cys35 is found to exchange rapidly with the solvent in the oxidized but not in the reduced protein, at variance with H/D exchange experiments, which probe a different time scale. The present data confirm that electron-transfer proteins evolved to minimize reorganization energy upon change of the oxidation state, even though the consequent variation of charge of the metal ion may induce some changes in the structure and/or dynamics of the protein.

The interaction of a protein with water molecules can occur in a number of ways, from very specific population of internal cavities to quite aspecific interactions at the protein surface. The lifetimes of these interactions are quite different (*1*). Protein hydration can be studied with a variety of techniques. X-ray protein crystallography can provide detailed information on the presence of ordered water molecules interacting with the protein in the crystal. However, little information on their lifetime is obtained. Information on the occupancy of interaction sites can also be lost at times (*2*, *3*). Hydration of proteins can be directly investigated by nuclear magnetic resonance dispersion (*4*). This technique, however, cannot provide high-resolution information on where specific protein-water interaction sites are located. Finally, high-resolution NMR[1] spectroscopy can provide information on the presence of water molecules at atomic level, as well as on their lifetimes, provided that the latter are in a suitable range (*5*).

The interaction between the polypeptide chain and the solvent is very often crucial for both the biological function and the thermodynamic stability of proteins. Metalloproteins comply with this general behavior; for example, the dramatic influence of solvent accessibility on the redox potential of metal cofactors has been extensively documented (*6*−*10*). Furthermore, metalloproteins present the possibility of redox-state-dependent variations in the interaction with the solvent (along with a number of other properties (*11*, *12*)). Within this frame, *c*-type cytochromes probably constitute the largest and most studied family of metalloproteins. The largest bulk of data is available for mitochondrial cytochromes *c*, also thanks to the fact that crystal structures at a very good resolution have been available since the seventies (*13*). Systematic investigations at the atomic level on the relationship between redox state and protein hydration in *c*-type cytochromes have been performed mainly through X-ray crystallography (*14*−*18*) and molecular dynamics simulations (*19*). ^{17}O nuclear magnetic resonance dispersion has quite recently been shown to be very useful in highlighting redox-dependent variations of protein hydration (*20*). In addition, a few high-resolution ^{1}H NMR studies are also available for horse heart cytochrome *c* (*21*−*23*). Most articles dealing with redox-state dependent hydration of both bacterial and eukaryotic *c*-type cytochromes focused on the role of the so-called catalytic water, which is a buried water molecule observed in the proximity of the heme cofactor in the crystal structures and whose exact position and network of interactions with the protein moiety is a function of the oxidation state of the heme ion (*15*−*18*). This redox-dependent displacement was confirmed also by NMR spectroscopy on horse heart cytochrome *c* (*21*), although the position of the water molecule with respect to the heme in the oxidized protein appeared different in solution and in the crystal (*22*).

In this study, we have applied high-resolution NMR spectroscopy to investigate the interaction of a small bacterial cytochrome *c* with water and to analyze at the atomic level

[†] Financial support by MIUR (COFIN 2001) and by the European Commission (Contract QLG2-CT-1999-01003 to P.R.V., Contract Number HPRN-CT-2000-00092) is gratefully acknowledged.

* Corresponding author. Tel.: +39 055 4574272. Fax: +39 055 4574271. E-mail: bertini@cerm.unifi.it.

[‡] Magnetic Resonance Center (CERM).

[§] Department of Chemistry.

[1] Abbreviations: NMR, nuclear magnetic resonance; NOE, nuclear Overhauser effect; HSQC, heteronuclear single quantum correlation spectroscopy; *Bp*cytc, *Bacillus pasteurii* cytochrome c_{553}; CLEANEX, clean exchange; ePHOGSY, enhanced protein hydration observed through gradient spectroscopy; ROESY, nuclear Overhauser effect in the rotating frame spectroscopy; Tr-ROESY, transverse ROESY.

10.1021/bi0272961 CCC: $25.00
Published on Web 03/06/2003

protein−water interactions in both oxidation states of the heme iron ion. The system used in this work is the soluble fragment of the membrane-anchored *Bacillus pasteurii* cytochrome *c* (*Bp*cyt*c* hereafter), which features stable iron His/Met coordination over the pH range 1−12 and up to 70 °C (*24*). This is most likely linked to the fact that *Bacillus pasteurii* is a gram-positive alkaliphilic and highly ureolytic soil bacterium, which grows optimally at pH 9.2 in the presence of ammonium salts (*25*) or urea (*25*−*28*). *Bp*cyt*c* is a 71-amino acid protein and thus has one of the lowest amino acid-to-heme ratios ever reported for monoheme *c*-type cytochromes (*29*), making it a "minimal" cytochrome *c*. The oxidized protein has been structurally characterized under native conditions by X-ray crystallography (*30*) and NMR spectroscopy (*31*), while a NMR structure is available for the reduced protein (*32*). The dynamical properties of the *Bacillus pasteurii* protein on the experimentally accessible time scales have been also characterized by means of NMR experiments in both oxidation states (*31*, *32*). Finally, details are available for the equilibrium unfolding of oxidized *Bp*cyt*c* in guanidinium, which have provided hints on the structural determinants of thermodynamic stability of this class of proteins (*33*). The methodology employed here is based on the use of selective excitation of the water signal followed by the acquisition of $^{1}H-^{15}N$ correlation spectra to detect water molecules interacting with the amide protons of the protein. Water−protein magnetization transfer that can be detected by this approach is mediated by both dipolar interaction and chemical exchange; combining different experiments allowed us to assess the relative importance of these two mechanisms.

It is found that in the present system there are no redox-dependent variations in the interaction between the protein moiety and long-lived water molecules. On the other hand, a redox-state-independent water molecule is identified, whose key interactions with the protein suggest a reason for the observed (*24*, *33*) enhanced stability of the axial coordination of the iron ion. It is apparent that carefully designed interactions between water molecules and amino acids are key to stabilizing the environment of bound cofactors. A redox dependent behavior is observed for fast chemical exchange between amide groups and bulk solvent.

MATERIALS AND METHODS

All the 2D experiments were performed at 11.7 T on a Bruker 500 Avance spectrometer equipped with a cryoprobe: CLEANEX (*34*), Tr-ROESY (*35*), and ePHOGSY with a flip-back pulse (*36*) using HSQC detection combined with WATERGATE to suppress water. Samples of 0.5−1.5 mM fully ^{15}N enriched *Bacillus pasteurii* cytochrome *c* samples were used, at pH 6.0, in both the oxidized and the reduced state. Sample preparation was done as previously described (*31*), with the only exception being that 100 mM phosphate buffer was used. The protein was reduced with an excess of dithionite, added anaerobically (*32*). The experiments were performed at 23 °C.

The pulse used for selective water excitation was a 7.5 ms long 180° Gaussian pulse. Pulses of 22.5 and 30 ms were also used in order to increase the selectivity and discriminate between water and Hα resonances. Before and after the selective pulse, sine-shaped gradients with a maximum intensity of 7 G/cm were applied. A gradient recovery delay of 0.2 ms was used after the pulsed field gradients. The mixing time was 80 ms, the spin-lock pulses were applied at an r.f. frequency of 5.1 kHz, and a weak gradient was maintained during the mixing time in order to avoid radiation damping effects. Thirty-two scans were recorded, and a data matrix of 2k × 128 points was collected and transformed to 1k × 256 points. The relaxation delay was set to 1.5 s, and the acquisition time was 124 ms. The spectral windows used were 16.5 ppm for the proton and 35 ppm for the nitrogen, with the carrier set at the water frequency (4.74 ppm) and at 118 ppm, respectively. To distinguish, on the basis of the different relaxation properties, between magnetization originating from water and magnetization originating from protein protons, a series of experiments were acquired in which a spin−echo of variable duration had been inserted at the beginning of the Tr-ROESY experiment. The use of spin−echo relaxation filters has been previously described in the literature (*37*, *38*), albeit with a less quantitative approach than what used here. The duration of the spin−echo was varied in the range 0−180 ms. Thanks to the use of a selective 180° pulse in the spin−echo, the intensities measured in the 2D spectra could be fitted to an exponential decay with two parameters (*5*). The relaxation rates resulting from the fit are, to a good approximation (the contribution due to diffusion is estimated well below 1 s^{-1}), the transverse relaxation rates of the protons transferring magnetization to the detected amides. The exchange rates of protons were fitted by recording a series of spectra with various mixing times in CLEANEX, ranging from 5 to 35 ms and by fitting the ratio of peak intensities in the CLEANEX spectra recorded to the intensity in a reference HSQC spectrum. The equation used was (*34*)

$$\frac{I_{\mathrm{Cl}}(t_{\mathrm{m}})}{I_{\mathrm{HSQCref}}} = \frac{k}{R_{1\mathrm{A}} + k - R_{1\mathrm{B}}} \times [\mathrm{e}^{-R_{1\mathrm{B}}t_{\mathrm{m}}} - \mathrm{e}^{-(R_{1\mathrm{A}} + k)t_{\mathrm{m}}}]$$

where R_{1A} is the relaxation rate under CLEANEX mixing conditions (a combination of transverse and longitudinal relaxation), R_{1B} is the water relaxation rate during the mixing time, and k is the exchange rate. The water relaxation rate has been found to be very small (practically the variation of the water signal by using a mixing time of 5 or 120 ms is undetectable). A value for R_{1B} of 0.01 s^{-1} has been used (varying this value between 0.1 and 0.001 gives no difference in the k values obtained from the fit).

Spectra were acquired and processed using XWinNMR 3.1 and analyzed using Sparky. Data were fitted using Sparky modules and Matlab version 6.1 for Linux.

The structures used for analysis were the X-ray structure and the NMR solution structure of the oxidized protein (PDB entries 1C75 and 1K3H, respectively), and the NMR solution structure of the reduced protein (PDB entry 1N9C).

RESULTS

The general strategy of the three experiments performed is to selectively excite the magnetization of the solvent and then observe the signals of amide groups whose magnetization has been brought out of equilibrium because of their interaction with the solvent molecules. This can happen through two mechanisms: dipolar interaction (that is, NOE) or chemical exchange. In the CLEANEX experiment, the

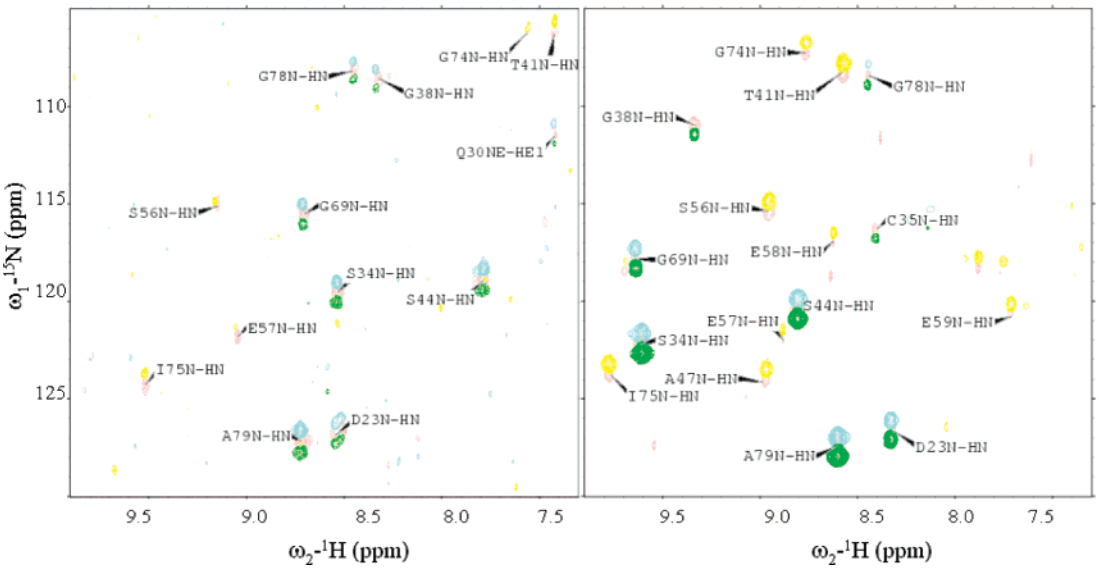

FIGURE 1: Comparison of CLEANEX (green), Tr-ROESY (yellow: negative peaks, cyan positive peaks), and ePHOGSY (red) spectra for reduced (left) and oxidized (right) *Bp*cyt*c*. The CLEANEX and Tr-ROESY spectra have been offset for better vision.

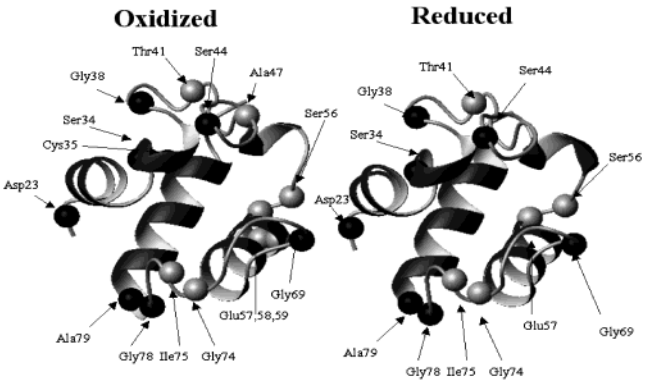

FIGURE 2: Backbone amide groups displaying interaction with water molecules in oxidized and reduced *Bacillus pasteurii* cytochrome *c* (shown using ribbon display). Light gray spheres represent amide groups which generate negative intensity in Tr-ROESY experiments and no or very weak signal in CLEANEX. Dark gray spheres represent amide groups interacting via chemical exchange (positive intensity in CLEANEX).

dipolar interaction is suppressed, and only amide protons exchanging with water are detected (*34*, *39*). In the Tr-ROESY experiment instead, both mechanisms are operative and give rise to magnetization of the amide protons of opposite sign (*35*). Finally, in the ePHOGSY-HSQC experiment, both mechanisms are again operative but now give rise to magnetization of the amide protons of the same sign (*36*).

Figure 1displays an overlay of the spectra obtained for oxidized *Bp*cyt*c*. The distribution along the polypeptide chain of the amide groups showing interaction with water is depicted in Figure 2. In oxidized *Bp*cyt*c*, eight positive signals were identified in the CLEANEX experiment, while seven were identified in the reduced species (Figure 2). As expected, they all correspond to signals that could not be detected in an HSQC spectrum taken 10 min after dissolving the protein in D_2O (*31*, *32*). Indeed, the exchange rates for the amide protons of the residues observed in CLEANEX are in the range 0.1−3.5 s^{-1}, with the highest rates in the oxidized protein belonging to Ser34 and Ala79 (3 and 3.5 s^{-1}, respectively). Figure 2 shows that these residues, with the exception of Ser34 and Cys35, belong to solvent-exposed protein loops.

The ePHOGSY spectrum of the oxidized species additionally shows eight backbone amide groups signals due to mainly dipolar interactions: Thr41, Ala47, Ser56, Glu57, Glu58, Glu59, Gly74, and Ile75 (Figure 2). Five amide groups with analogous characteristics are identified in the reduced species: Thr41, Ser56, Glu57, Gly74, and Ile75 (Figure 2). The Tr-ROESY spectra show the same signals of the ePHOGSY spectra (but Gly38 in the oxidized protein, see below), with positive peaks for the signals observed in the CLEANEX experiments and negative peaks for the additional signals showing up in the ePHOGSY spectra. At this point, it is useful to note that the present approach does not allow an easy distinction between signals arising due to the dipolar interaction between amide protons and water molecules and signals due to NOE transfer from Hα protons resonating close to the water frequency or from protons in rapid exchange with water. Inserting a relaxation filter into the sequence, as described in Materials and Methods, solved this ambiguity. The much shorter relaxation rates of protein protons allow differentiation of signals due to intramolecular interactions from signals due to protein−solvent interactions (*37*, *38*). Figure 3 reports the relaxation rates obtained for all signals detected in Tr-ROESY experiments. The first information that becomes apparent from Figure 3 is that the relaxation times of both water and protein protons are shorter in the system containing the oxidized (paramagnetic) protein. All signals arising due to exchange with water have relatively long relaxation times in the modified Tr-ROESY pulse scheme, consistent with them being originated by interaction with water molecules.

The signal from the amide group of Ala47 is already lost when a delay of 50ms is inserted before and after the selective pulse. Its short relaxation time indicates that the origin of magnetization is the Hα proton of Pro46, which is 2.4 Å away in the X-ray structure and which resonates very close to the frequency of water (4.74 ppm). The amide group of Ala47 is not detected for reduced *Bp*cyt*c*, as the resonance of the Hα proton is shifted by 0.8 ppm upon reduction.

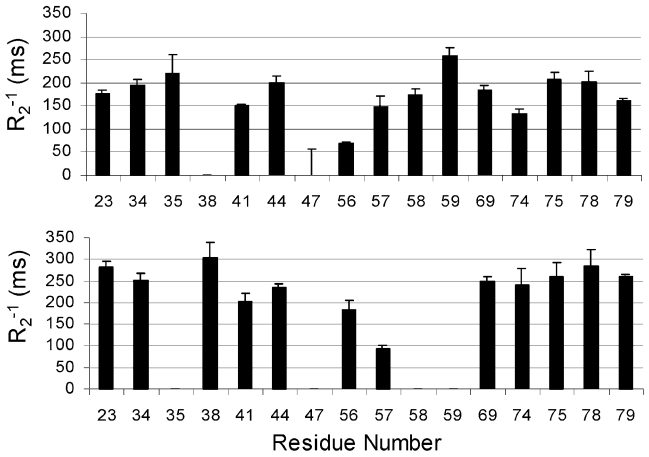

FIGURE 3: Relaxation times resulting from the Tr-ROESY experiment by inserting a relaxation delay in the water-selection scheme in oxidized (top) and reduced (bottom) *Bp*cyt*c*. In the oxidized protein, the signal of Gly38 is not detected in Tr-ROESY experiments (see text).

The amide moiety of Thr41, observed with opposite sign in the ePHOGSY and Tr-ROESY experiments, is within hydrogen bond distance from the hydroxyl group of the same residue in the atomic resolution X-ray (*30*) and the NMR structures of both oxidized (*31*) and reduced *Bp*cyt*c* (*32*, *32*). Thus, it is possible that for this residue we are detecting an NOE to the hydroxyl group.

NOE transfers to amide atoms in residues 56−59 are possibly arising from interaction with the hydroxyl group of Ser56 and/or the Hα protons of residues 55 and 56, which in both oxidation states resonate within 0.2 ppm from the water frequency. In the X-ray structure (*30*), the amide moiety of Glu59 is hydrogen-bonded to the hydroxyl group of Ser56; this hydrogen bond is present also in some conformers of the NMR family (*31*). In the majority of the conformers of the NMR structure, the amide proton of Glu59 is within 3 Å from the hydroxyl group of Ser56 (*31*). In the reduced protein, the side chain of Ser56 moves away from Glu58 and Glu59 (*32*); this displacement may thus be responsible for the different behavior of Glu58 and Glu59 in the two oxidation states. Interestingly, the decrease in the relaxation time of the amide group of Glu57 upon reduction (Figure 3) is also consistent with a decreased interaction with the Ser56 hydroxyl group, again due to the increased distance between the two moieties in reduced with respect to oxidized *Bp*cyt*c*. Indeed, such a reduced interaction would make the interaction of the amide group of Glu57 with the Hα proton of residue 56 the dominant mechanism for magnetization transfer in the reduced state. Consistent with this, an increase in the length of the selective pulse in the Tr-ROESY experiment results in significant variations of the intensities of signals of E56 and E57, indicating a significant contribution from interaction with a proton resonating close to but not exactly in overlap with the water signal.

In oxidized *Bp*cyt*c*, the signal of Gly38 was observed in the CLEANEX spectrum, but not in the Tr-ROESY; this can be due to the fact that the exchange and dipolar contribution are of opposite sign and, if simultaneously present, can thus cancel out. A dipolar contribution for Gly38 in the oxidized protein can result from interaction with the Hα1 proton of Gly37, which resonates very close to the water frequency.

Table 1: Selected Structural Parameters for the Long-Lived Water Molecule Identified by NMR in the Present Work, Calculated on the Basis of the Position of Wat95 in the High-resolution X-Ray Structure of *Bp*cyt*c* (PDB entry 1C75) (*30*)

parameter	value
distance O(Wat95)−HN(Ile75)	2.06 Å
angle O(Wat95)−HN(Ile75)−N(Ile75)	161°
distance O(Wat95)−HN(Gly74)	3.22 Å
distance O(Wat95)−O(Pro72)	2.79 Å
distance O(Wat95)−O(Ile64)	2.66 Å
distance O(Wat95)−Fe	6.76 Å

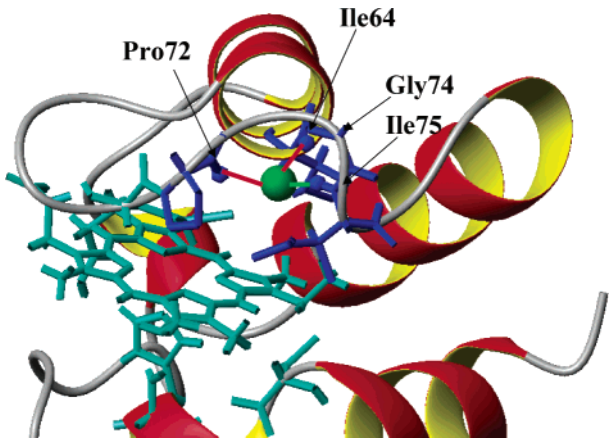

FIGURE 4: Close-up view of the water molecule (Wat95) present in the X-ray structure of oxidized *Bp*cyt*c* (PDB entry 1C75 (*30*)), whose presence in solution in both oxidation states has been evidenced by the present investigation. The network of hydrogen bonds involving the water molecule is shown (green line, H-bond between the amide group of Ile75 and the water oxygen; red lines, possible H-bonds between the water hydrogen atoms and the oxygen atoms of the carbonyl moieties of Ile64 and Pro72).

The data obtained in the present work provide clear-cut evidence that there is a NOE interaction with water protons for the amide protons of Gly74 and Ile75 in both oxidation states (Figures 2 and 3). Indeed, the signals of these two amide groups are absent in CLEANEX spectra and have a positive signal in ePHOGSY spectra and negative signal in Tr-ROESY spectra, implying that they are involved in a pure dipolar interaction with a water proton, with a negative NOE transfer rate. The amide groups of both residues are completely shielded from the bulk solvent, suggesting that a water molecule is internalized in this region of the protein. The negative NOE observed for the amide protons of Gly74 and Ile75 is consistent with an overall correlation time for the interaction larger than 0.36 ns. By assuming isotropic rotation of the protein (*31*), the absence of local mobility, and a two-site exchange of the water molecule (*5*), a residence time τ_m of the water molecule larger than 0.4 ns can be derived, as otherwise it would become the correlation time for the reorientation and the NOE's would be positive. ^{17}O NMRD data (not shown) suggest that τ_m is actually longer than the correlation time for rotation of the protein in solution (3.6 ns (*31*)). A water molecule in a position suitable to give rise to the observed NOE's can be identified in the X-ray structure and corresponds to Wat95. Its oxygen atom is 2.1 Å away from the amide proton of Ile75, i.e., at H-bond distance (Table 1 and Figure 4); consistent with its presently observed long residence time, Wat95 features a quite low temperature factor. Structure calculations (not shown) run with the program DYANA (*40*) using all the

constraints available for oxidized *Bp*cyt*c* (*31*), and including a single water molecule constrained within 3.5 Å from the HN atoms of Gly74 and Ile75 result in a family of conformers essentially indistinguishable from that obtained without inclusion of the water molecule, where the latter is indeed internalized in a position superimposable to that of Wat95. The bulky side chain of Ile75 significantly contributes to segregating Wat95 from the bulk solvent. The present data and the inspection of the X-ray structure suggest that the orientation of the water molecule is such that its protons could form an hydrogen bond with the carbonyl oxygen of Pro72 and possibly also with that of Ile64.

DISCUSSION

NMR Spectroscopy. The methodology used to separate the individual contributions of dipolar cross-relaxation and chemical exchange to the overall intensity of the protein signals detected traditionally relies on recording two spectra alternatively exploiting magnetization transfer between spins aligned with the main field or in the rotating frame (*1*, *41*). If the correlation time of the interaction is longer than a certain threshold, the rate of dipolar transfer changes sign in the two spectra with respect to the exchange rate (*5*). When the two mechanisms of magnetization transfer occur simultaneously, the comparison of the two spectra allows one to identify the dominant effect. In our approach, a third spectrum specifically aimed at the selective detection of signals arising from exchange contributions (*34*) has been recorded. This permits separating peaks that are exclusively due to dipolar interaction between water and protein protons (even through a relay mechanism) from peaks in which both magnetization transfer mechanisms are present without having to measure the individual transfer rates. The peaks that are essentially free from chemical exchange contributions and have a negative NOESY transfer rate make it possible to estimate a lower limit for the water residence time.

The only difference in the results of CLEANEX experiments between the oxidized and reduced *Bp*cyt*c* occurs at the position of Cys35. This variation is not related to a variation in solvent accessibility, as comparison of the NMR structures of the oxidized and reduced protein displays a difference in the accessibility of the amide proton of Cys35 of only 2%. The slowed chemical exchange of Cys35 in the reduced state parallels the general behavior observed through H/D exchange experiments for the present (*32*) as well as a number of other *c*-type cytochromes (*42*−*45*), where the backbone amide moieties of residues in regions with regular secondary structure exchange significantly faster in the oxidized with respect to reduced state. These exchange processes take place on time scales ranging from minutes to days, i.e., much slower than the time scale addressed by CLEANEX experiments. It is to be noted that CLEANEX data provide a less clear-cut differentiation between the two oxidation states, probably because they monitor mainly exchange in unprotected regions of the structure, which is always fast.

No significant differences with respect to the presence of long-lived water molecules were observed between the two physiologically relevant oxidation states of *Bp*cyt*c*. Indeed, only one such water molecule could be detected through our approach (Figure 4), whose position is not affected by changes in the oxidation state of the iron ion. Variation in the oxidation state, and thus charge, of the metal center results in the variation of the electrostatic interaction energy between the latter and the water molecule. This could lead to redox-state-dependent rearrangements in the position of the water molecule. However, the observed absence of structural changes indicates that the energetics of the network of H-bonds (Table 1 and Figure 4) involving this water molecule is such that variations in its position (which would require at least partial disruption of this network) are prevented.

The present findings further contribute to the bulk of evidence indicating that in general electron-transfer protein experience little redox state-dependent variation of their structural and dynamic properties (*32*, *42*, *45*−*52*). Perhaps more importantly, these variations appear to be significantly different not only for different kinds of electron-transfer proteins (i.e., blue copper proteins vs ferredoxins vs cytochromes), but even within an individual class of electron-transfer proteins (i.e. *c*-type cytochromes) in terms of both amplitude and location within the protein frame of the changes. As discussed in detail in the next section, this holds true also for long-lived water molecules, whose position, in *c*-type cytochromes, may or may not experience redox-state rearrangements, depending on the specific cytochrome investigated. Even though a broad general trend can be identified, that is, electron-transfer proteins sample the conformational space to different extents in different oxidation states (*32*, *51*), the available data suggest that the protein structure and dynamics are evolved in order to minimize the consequences of the variation of the charge of the metal cofactor implied by the electron transfer process. The charge variation of the metal site may still induce variations of some kind in the protein structural/dynamic properties, whose precise nature clearly depends on the system taken into consideration. Intriguingly, there are indications that more evolved systems (e.g., mitochondrial *c*-type cytochromes) allow larger redox state-dependent variations, as if Nature developed some use for these effects along the course of evolution.

The Role of Long-Lived Water Molecules in c-Type Cytochromes. Extensive literature is available on the presence and redox-dependent features of internal water molecules in *c*-type cytochromes, particularly for mitochondrial (*14*, *15*, *21*, *53*) and the similar c_2 bacterial cytochromes (*17*, *18*). For oxidized horse heart cytochrome *c*, there is good agreement between data obtained from the X-ray structure and NMR data on protein−water interactions in solution (*21*−*23*). Data are also available for cytochrome c_6 from the alga *Scenedesmus obliquus* (*16*). In the mitochondrial, c_2, and algal proteins, a water molecule in essentially the same position with respect to the heme cofactor is detected. In several but not all of these systems, the mentioned water molecule experiences a redox-dependent displacement, and for this reason has often been dubbed "catalytic". It has been proposed that this displacement could lower the redox potential of the iron ion by about 100 mV (*54*). The presence or absence of this behavior has been related to subtle differences in the hydrogen bond network involving the water molecule (*54*).

In *Bp*cyt*c*, there is no water molecule equivalent to the above-mentioned catalytic water of mitochondrial, c_2, and

c_6 cytochromes (*30*). This difference is possibly related, at least in part, to the significantly higher solvent accessibility of the heme cofactor in the present system. On the other hand, the long-lived internal water molecule identified here, whose position appears to have little, if any, dependence on the redox state, appears to have no equivalent in the other mentioned systems. The long-lived water of *Bp*cyt*c* is at the heart of a network of H-bond interactions connecting the axial Met loop to the long α-helix spanning residues 57−66. This unique structural feature could be responsible for the observed enhanced stability with respect to mitochondrial cytochromes of the iron axial coordination in *Bp*cyt*c* toward alkaline pH (*24*) and denaturants (*33*). This enhanced stability is likely linked to the requirements caused by the relatively harsh environment to which *Bp*cyt*c* is exposed in vivo (pH 9.2 and urea-rich (*27*)). Indeed, the detailed investigation of the equilibrium unfolding of oxidized *Bp*cyt*c* indicates that this process is characterized by the presence of a trigger mechanism, by which a single event at molecular level induces detachment of the axial Met from the iron(III) ion and unfolding of large part of the polypeptide chain (*33*). The present data suggest that this event may be related to loss of the internal water molecule identified here and the consequent disruption of the long-range H-bond network of Figure 4.

Overall, it appears that a generalization of the role of internal water molecules in *c*-type cytochromes is not possible. On the contrary, it appears that such water molecules are used by Nature in different ways, to tune different structural and functional aspects. Structurally equivalent internal water molecules, but with different functional properties, are found in cytochromes which are evolutionarily close (*16*−*18*, *54*), suggesting that the presence and location of buried water molecules may be selected by evolution.

Considerations on the Redox Potential. Horse heart cytochrome *c* has been shown to release one immobilized water molecule to the bulk solvent upon reduction (*20*), providing an increase in the entropy of reduction (*55*). Still, experimental data clearly show that the entropy of reduction is negative (−120.8 J mol^{-1} K^{-1}) (*56*). It is therefore necessary to assume that other processes provide a larger in magnitude, negative contribution to the entropy of reduction. It appears likely that this contribution arises from the more restricted flexibility of the reduced versus oxidized protein (*47*, *50*). The present data for *Bp*cyt*c* indicate that there is no release of the only immobilized water molecule detected upon reduction. The entropy of reduction of *Bp*cyt*c* is slightly more negative than that of mitochondrial cytochromes *c* (−162.7 J mol^{-1} K^{-1} (*24*)). In keeping with this observation, the reduced protein is less flexible than the oxidized, in particular on the time scale of the minute and longer (*32*). The available data suggest that the conformational space sampled by *Bp*cyt*c* or mitochondrial cytochromes *c* is somewhat smaller in the reduced with respect to the oxidized state, which could be also of functional importance (*32*). The significantly different size and primary sequence of *Bp*cyt*c* and typical mitochondrial cytochromes *c* prevent a quantitative comparison of the various contributions to the entropy of reduction. Nevertheless, it appears that generally the entropy of reduction of cytochromes is determined primarily by the number of conformational substates that the polypeptide chain can span in solution in each oxidation state. Variations in protein hydration likely contribute to a somewhat smaller extent (*20*).

As far as the enthalpic contribution of the presence of internal water molecules is concerned, the investigation of the solid-state structures of a number of mitochondrial cytochromes *c* and bacterial cytochromes c_2 indicated that the long-lived "catalytic" water molecule present in this systems can lower by up to 100 mV the reduction potential by stabilizing the oxidized form of the protein through a redox-state dependent structural rearrangement (*54*). This contribution is absent in the present system, whose enthalpy of reduction is significantly lower than in the case of the other aforementioned *c*-type cytochromes; this finding is ascribed to the higher solvent accessibility of the heme moiety (*24*, *30*). Calculations of the redox potential with the program DelPhi (*57*) indicate that the mere presence of the long-lived water identified in this work results in an essentially negligible contribution to the reduction potential of *Bp*cyt*c*. This constitutes a further indication that this water molecule plays a structural rather than functional role, as it has instead been proposed for the catalytic water of mitochondrial cytochromes *c*.

CONCLUSIONS

In the present work, we have performed a high-resolution NMR study of the interaction between water and a small bacterial cytochrome *c* in both the physiologically relevant oxidation states. Redox-state dependent effects were found to be limited to a difference in the exchange rate of the backbone amide moiety of Cys35, consistent with the pattern observed for exchange rates in the minute and longer time scale (*32*). A single long-lived water molecule was detected, in a position analogous to that of Wat95 in the X-ray structure of oxidized *Bp*cyt*c* (PDB code 1C75) (*30*). Its position did not change appreciably upon reduction, suggesting that the network of H-bonds involving it (Figure 4) is energetically quite stable.

The comparison of the present data obtained for *Bp*cyt*c* with the data available in the literature for mitochrondrial cytochromes *c* and bacterial cytochromes c_2 indicates that the biological role of long-lived water molecules in *c*-type cytochromes is quite variable. In the latter, more complex cytochromes, some structurally homologous internal waters have been identified, for which a functional role has been proposed in modulating the reduction potential, probably by affecting mostly the enthalpy of reduction (*14*, *15*, *17*, *18*, *54*). However, even this is not a general behavior (*16*). In *Bp*cyt*c*, which belongs to a different subfamily of *c*-type cytochromes (*58*), the only long-lived water molecule that could be identified occupies a position with no equivalent in the other systems mentioned. The present data, together with the results of equilibrium unfolding studies (*33*), strongly suggest that the biological role of this water molecule is a structural rather than functional one, by forming key hydrogen-bonds, which hold together the loop region of axial Met and the C-terminal part of the long helix α_4. It can thus be concluded that water−protein interactions in *c*-type cytochromes constitute a very versatile means by which Nature can optimize either the structural or functional properties of the metalloprotein.

ACKNOWLEDGMENT

We thank Ilaria Bartalesi for help in sample preparation and Kirill Nerinovski for NMRD measurements.

REFERENCES

1. Otting, G., Liepinsh, E., and Wüthrich, K. (1991) *Science 254*, 974−980.
2. Baker, E. N. (1995) in *Protein−Solvent Interactions* (Gregory, R. B., Ed.) M. Dekker, New York.
3. Schoenborn, B. P., Garcia, A., and Knott, R. (1995) *Prog. Biophys. Mol. Biol. 64*, 105−119.
4. Halle, B., Denisov, V. P., and Venu, K. (1999) *Biol. Magn. Reson. 17*, 419−483.
5. Otting, G. (1997) *Prog. NMR Spectrosc. 31*, 259−285.
6. Langen, R., Brayer, G. D., Berghuis, A. M., McLendon, G. L., Sherman, F., and Warshel, A. (1992) *J. Mol. Biol. 224*, 589−600.
7. Battistuzzi, G., Borsari, M., Sola, M., and Francia, F. (1997) *Biochemistry 36*, 16247−16258.
8. Capozzi, F., Ciurli, S., and Luchinat, C. (1998) *Struct. Bonding 90*, 127−160.
9. Springs, S. L., Bass, S. E., Bowman, G., Nodelman, I., Schutt, C. E., and McLendon, G. L. (2002) *Biochemistry 41*, 4321−4328.
10. Battistuzzi, G., Borsari, M., Cowan, J. A., Ranieri, G. A., and Sola, M. (2002) *J. Am. Chem. Soc. 124*, 5315−5324.
11. Bertini, I., Rosato, A., and Turano, P. (1999) *Pure Appl. Chem. 71*, 1717−1725.
12. Banci, L., Bertini, I., Luchinat, C., and Turano, P. (2000) in *The Porphyrin Handbook* (Kadish, K. M., Smith, K. M., and Guilard, R., Eds.) pp 323−350, Academic Press, San Diego, CA.
13. Swanson, R., Trus, B. L., Mandel, N., Mandel, G., Kallai, O. B., and Dickerson, R. E. (1977) *J. Biol. Chem. 252*, 759−775.
14. Berghuis, A. M., and Brayer, G. D. (1992) *J. Mol. Biol. 223*, 959−976.
15. Berghuis, A. M., Guillemette, J. G., McLendon, G. L., Sherman, F., Smith, M., and Brayer, G. D. (1994) *J. Mol. Biol. 236*, 786−799.
16. Schnackenberg, J., Than, M. E., Mann, K., Wiegand, G., Huber, R., and Reuter, W. (1999) *J. Mol. Biol. 290*, 1019−1030.
17. Sogabe, S., and Miki, K. (2001) *FEBS Lett. 491*, 174−179.
18. Geremia, S., Garau, G., Vaccari, L., Sgarra, R., Viezzoli, M. S., Calligaris, M., and Randaccio, L. (2002) *Protein Sci. 11*, 6−17.
19. Banci, L., Gori Savellini, G., and Turano, P. (1997) *Eur. J. Biochem. 249*, 716−723.
20. Bertini, I., Hajieva, P., Luchinat, C., and Nerinovski, K. (2001) *J. Am. Chem. Soc. 123*, 12925−12926.
21. Qi, P. X., Urbauer, J. L., Fuentes, E. J., Leopold, M. F., and Wand, A. J. (1994) *Nat. Struct. Biol. 1*, 378−382.
22. Bertini, I., Dalvit, C., Huber, J. G., Luchinat, C., and Piccioli, M. (1997) *FEBS Lett. 415*, 45−48.
23. Bertini, I., Huber, J. G., Luchinat, C., and Piccioli, M. (2000) *J. Magn. Reson. 147*, 1−8.
24. Benini, S., Borsari, M., Ciurli, S., Dikiy, A., and Lamborghini, M. (1998) *J. Biol. Inorg. Chem. 3*, 371−382.
25. Wiley, W. R., and Stokes, J. L. (1963) *J. Bacteriol. 86*, 1152−1156.
26. Larson, A. D., and Kallio, R. E. (1954) *J. Bacteriol. 68*, 67−73.
27. Bornside, G. H., and Kallio, R. E. (1956) *J. Bacteriol. 71*, 627−634.
28. Wiley, W. R., and Stokes, J. L. (1962) *J. Bacteriol. 84*, 730−734.
29. Barker, P. D., and Ferguson, S. J. (1999) *Struct. Folding Des. 7*, R281−R290.
30. Benini, S., Rypniewski, W., Wilson, K. S., Van Beeumen, J., and Ciurli, S. (2000) *Biochemistry 39*, 13115−13126.
31. Banci, L., Bertini, I., Ciurli, S., Dikiy, A., Dittmer, J., Rosato, A., Sciara, G., and Thompsett, A. (2002) *ChemBioChem 3*, 299−310.
32. Bartalesi, I., Bertini, I., and Rosato, A. (2003) *Biochemistry 42*, 739−745.
33. Bartalesi, I., Bertini, I., Ghosh, K., Rosato, A., and Turano, P. (2002) *J. Mol. Biol. 321*, 693−701.
34. Hwang, T. L., Van Zijl, P. C. M., and Mori, S. (1998) *J. Biomol. NMR 11*, 221−226.
35. Hwang, T. L., and Shaka, A. J. (1995) *J. Magn. Reson. A 112*, 275−279.
36. Dalvit, C. (1996) *J. Magn. Reson. Ser. B 112*, 282−288.
37. Mori, S., Berg, J., and Van Zijl, P. C. M. (1996) *J. Biomol. NMR 7*, 77−82.
38. Dalvit, C., Floersheim, P., Zurini, M., and Widmer, A. (1999) *J. Biomol. NMR 14*, 23−32.
39. Hwang, T. L., Mori, S., Shaka, A. J., and Van Zijl, P. C. M. (1998) *J. Am. Chem. Soc. 119*, 6203−6204.
40. Güntert, P., Mumenthaler, C., and Wüthrich, K. (1997) *J. Mol. Biol. 273*, 283−298.
41. Otting, G., and Wüthrich, K. (1989) *J. Am. Chem. Soc. 111*, 1871−1875.
42. Banci, L., Bertini, I., Bren, K. L., Gray, H. B., Sompornpisut, P., and Turano, P. (1997) *Biochemistry 36*, 8992−9001.
43. Baxter, S. M., and Fetrow, J. S. (1999) *Biochemistry 38*, 4493−4503.
44. Banci, L., Bertini, I., De la Rosa, M. A., Koulougliotis, D., Navarro, J. A., and Walter, O. (1998) *Biochemistry 37*, 4831−4843.
45. Reincke, B., Perez, C., Pristovsek, P., Lucke, C., Ludwig, C., Lohr, F., Ludwig, B., and Ruterjans, H. H. (2001) *Biochemistry 40*, 12312−12320.
46. Banci, L., Bertini, I., Cavazza, C., Felli, I. C., and Koulougliotis, D. (1998) *Biochemistry 37*, 12320−12330.
47. Fetrow, J. S., and Baxter, S. M. (1999) *Biochemistry 38*, 4480−4492
48. Arnesano, F., Banci, L., Bertini, I., Felli, I. C., and Koulougliotis, D. (1999) *Eur. J. Biochem. 260*, 347−354.
49. Banci, L., Bertini, I., Gray, H. B., Luchinat, C., Reddig, T., Rosato, A., and Turano, P. (1997) *Biochemistry 36*, 9867−9877.
50. Barker, P. B., Bertini, I., Del Conte, R., Ferguson, S. J., Hajieva, P., Tomlinson, E. J., Turano, P., and Viezzoli, M. S. (2001) *Eur. J. Biochem. 268*, 4468−4476.
51. Pochapsky, T. C., Kostic, M., Jain, N., and Pejchal, R. (2001) *Biochemistry 40*, 5602−5614.
52. Bertini, I., Bryant, D. A., Ciurli, S., Dikiy, A., Fernández, C. O., Luchinat, C., Safarov, N., Vila, A. J., and Zhao, J. (2001) *J. Biol. Chem. 276*, 47217−47226.
53. Lett, C. M., Berghuis, A. M., Frey, H. E., Lepock, J. R., and Guillemette, J. G. (1996) *J. Biol. Chem. 271*, 29088−29093.
54. Garau, G., Geremia, S., and Randaccio, L. (2002) *FEBS Lett. 516*, 285−286.
55. Dunitz, J. D. (1994) *Science 264*, 670.
56. Bertrand, P., Mbarki, O., Asso, M., Blanchard, L., Guerlesquin, F., and Tegoni, M. (1995) *Biochemistry 34*, 11071−11079.
57. Gilson, M. K., Sharp, K. A., and Honig, B. (1987) *J. Comput. Chem. 9*, 327−335.
58. Ambler, R. P. (1991) *Biochim. Biophys. Acta 1058*, 42−47.

BI0272961